

# Comparison of Vertically and Horizontally Polarized Radar Antennas for Target Detection in Sea Clutter – An Experimental Study

Armin Parsa and Noah H. Hansen  
R&D Department  
Rutter Inc.  
St. John's, Newfoundland, Canada

**Abstract**—An experimental study of small target detection in sea clutter using vertically and horizontally polarized radar antennas is presented. The experimental study is performed to detect a person in water (PIW) and a fast rescue craft (FRC). The vertically and horizontally polarized X-band radar data were recorded simultaneously from a mobile radar platform located at Cape Spear, Newfoundland, Canada. Two commercial marine radars with grazing angles less than  $1^\circ$  were used. The analysis of the experimental data shows that the vertically polarized antenna is equally effective for detecting small targets at close range and low sea states as a horizontally polarized antenna.

## I. INTRODUCTION

Conventional marine navigation radars scan the ocean surface with HH (transmit and receive polarizations are horizontal) polarization. The HH polarization is thought to be superior to VV (transmit and receive polarizations are vertical) polarization due to its ability to suppress sea clutter and therefore increase the radar's ability to detect targets [1]. Recently, vertically (VV) polarized radar antennas are starting to be used for special applications such as oil spill detection and wave spectra analysis. This is due to evidence that the VV radar performs better than the HH radar in these special applications [2-4]. It would be useful for these special application radars to also be able to perform target detection tasks and therefore it is important to know their target detection capability.

The most demanding targets to detect in sea clutter are very small stationary targets such as a person in water (PIW) and small fast moving targets such as fast rescue craft (FRC). A floating target such as a PIW regularly becomes invisible on the radar screen when it is hidden behind a wave crest. Furthermore, a small fast target such as an FRC is constantly moving from scan to scan. As a result, both targets can easily be mistaken as sea clutter. These two types of targets are therefore used to compare the detection capability of HH and VV radar systems. The detection of a PIW and FRC depends on clutter intensity, range and radar system performance. Probability of detection is a widely accepted measure of radar

system performance in discrimination between the target and clutter signals [5-6].

This experimental study was performed to compare the ability of VV and HH polarized radars to detect small difficult targets in real life scenarios. The analysis was performed on PIW and FRC data recorded at Cape Spear, Newfoundland, Canada, when both HH and VV radars were working simultaneously. Using the recorded data, the probabilities of detection and of false alarm were obtained for the PIW and FRC for different scenarios. Furthermore, the effects of antenna rotation speed and scan-to-scan integration were also investigated.

The organization of this paper is as follows. Section II explains the method which is used for data analysis, and calculating the probabilities of detection and of false alarm. Section III presents the results obtained for the PIW and the FRC. Finally, Section III provides the conclusions.

## II. DATA ANALYSIS METHOD

The ability to distinguish the target echo signal from sea clutter and system noise defines the performance of a radar system. Radar performance is quantitatively defined by the Probability of Detection ( $P_d$ ) and the Probability of False Alarm ( $P_{fa}$ ). In order to calculate  $P_d$  and  $P_{fa}$  from the recorded data, two zones have been set up, namely target and clutter zones. The target zone is an area containing the target and it is chosen to be as small as possible so that radar returns other than from the target are not counted as target returns. The clutter zone includes an area much bigger than the target zone. Fig. 1 shows an example of a B-scan radar image with clutter and target zones. The red circle inside the target zone indicates a target hit, and the red circles inside the clutter zone indicate clutter hits. The groups of pixels that have intensities above the threshold level and are detected as a target by Sigma S6 Radar Processor [7] are referred to as "hits". The probability of false alarm is calculated using

$$P_{fa} = \frac{\text{clutter hits} - \text{targets hits}}{\text{clutter opportunity} - \text{target opportunity}} \times 100\%. \quad (1)$$

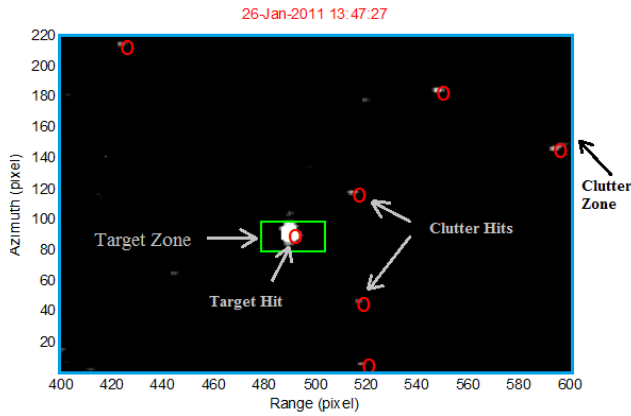


Figure 1. Clutter and target zones on a B-scan radar image. The radar image blobs are detected by the  $\sigma$  S6 plot extractor. The blob inside the target zone is counted as a target hit, and the blobs inside the clutter zone are counted as clutter hits.

The target and clutter opportunities are given by

$$\text{clutter opportunity} = n_c n_s \quad (2)$$

$$\text{target opportunity} = n_t n_s \quad (3)$$

where  $n_c$  and  $n_t$  are the numbers of clutter and target cells, and  $n_s$  is the number of scans used in the analysis. The number of clutter/target cells is the number of pixels inside the clutter/target zone area divided by the number of pixels inside a radar resolution cell. The radar resolution cell size is

$$\text{resolution cell} = c\tau/2R\theta \quad (4)$$

where  $c = 3 \times 10^8$  m/s (speed of light),  $\tau$  is the pulse length,  $R$  is the zone distance to the radar, and  $\theta$  is the 3-dB antenna beamwidth.

For the  $P_{fa}$  calculated in (1), the probability of detection is obtained using

$$P_d = [\text{target hits} - (P_{fa} n_t n_s)] / n_s \quad (5)$$

The precision of the  $P_d$  calculation is inversely proportional to the number of scans used in the calculations. As a rule of thumb, when the antenna rotation speed is 48 rpm, a minimum of two minutes of recording is needed to calculate the  $P_{fa}$  and  $P_d$  with sufficient precision.

For data analysis, Rutter's  $\sigma$  S6 software is used. The following steps are taken to calculate  $P_{fa}$  and  $P_d$ . First, a threshold value is chosen. The threshold values are relative numbers that are set by a radar adjustment. Second,  $P_{fa}$  and  $P_d$  are calculated by counting all the clutter and target hits for all the scans. If the calculated  $P_{fa}$  is not in the desired range

TABLE I. SEA CONDITION DURING THE FRC AND PIW TRIALS

Time (GMT)	Significant Wave height (m)	Wind Speed (knots)	Sea State
13:30	1.0	3.2	3
14:00	1.0	2.2	3
14:30	1.0	5.4	3
15:00	1.2	4.9	3
15:30	1.2	3.5	3



Figure 2. Rutter's mobile radar test platform equipped with the vertical and horizontal polarized radars.



Figure 3. Person in water close to Cape Spear site.

( $10^{-6} < P_{fa} < 10^{-4}$ ), the threshold is changed and the hits are counted again for all scans until the desired  $P_{fa}$  is obtained. The analysis usually requires changing the threshold and processing the data several times to obtain the desired  $P_{fa}$ .

### III. RESULTS

The PIW and FRC data recording was performed on January 26<sup>th</sup>, 2011. Two radars (Rutter Radar and Consilium) were used during this trial and both radars were transmitting and recording simultaneously. Fig. 2 shows the radar van which was used during the trial. The Rutter Radar system had an 8 ft. vertically polarized antenna prototype, while the Consilium system had a 9 ft. off-the-shelf horizontal polarized antenna. The horizontally and vertically polarized antennas had a beam width of 0.91 and 1 degree, respectively. The Consilium system was capable of 48, 60, 80 and 120 rpm antenna rotation rates. The Rutter Radar antenna

TABLE II. RADAR SYSTEMS SPECIFICATIONS

	HH (Consilium)	VV (Rutter Radar)
Antenna Gain (dB)	31	31
Antenna Beamwidth (degree)	0.91	1
Transmitter Peak Power (KW)	25	25
Operating Frequency (GHz)	9.375	9.41
Pulse Length (ns)	50	60
IF Bandwidth (MHz)	20	20
Overall Noise Figure (dB) $\leq$	5	5
Side Lobes (dB) $\leq$	-35	-30
PRF (Hz)	3000	3000

TABLE III. RADAR SETTINGS DURING THE PIW TRIAL

Run	Start Time (GMT)	Range (nmi)	Consilium Antenna Speed (rpm)	Rutter Radar Antenna Speed (rpm)
PIW.1	15:04	1.25	120	48
PIW.2	15:10	1.25	60	48
PIW.3	15:13	1.25	48	48
PIW.4	15:23	1.5	48	48
PIW.5	15:27	1.5	60	48
PIW.6	15:30	1.5	120	48

was only able to rotate at 48 rpm. The sea states during the trial were measured using a TRIAXYS Directional Wave buoy. The sea states obtained by the wave buoy and the radar specifications are shown in Table I and Table II, respectively.

A. Person in Water

The data recordings of the PIW were made at two target ranges, 1.25 and 1.5 nmi. Fig. 3 shows the person in water at 1.25 nmi. The Consilium radar recorded data at three different antenna rotation rates, 48, 60, and 120 rpm and the Rutter radar recorded data at one rotation rate, 48 rpm, as shown in Table III. The calculated values of  $P_{fa} / P_d$  and the thresholds used to obtain those values for the PIW trial are shown in Table IV, Table V, and Table VI. Also, the number of scans used to calculate the  $P_{fa} / P_d$  values are shown for each data set.

It should be noted that during the trial, sea birds were observed close to the PIW. The radar image blobs corresponding to the sea birds have a higher intensity level on HPOL radar images than on the VPOL images [8]. The recordings that had the most bird clutter were the recordings of the PIW at 1.5Nm. These scenarios are marked

TABLE IV. CALCULATED  $P_{fa}/Threshold/P_d$  FOR PIW.3 AND PIW.4 SCENARIOS

Run	PIW.3		PIW.4	
	1.25		1.5	
Range (nmi)	1.25		1.5	
Number of Scans used	130	130	97	97
Settings	VV	HH	VV	HH
Scans Averaged	48 rpm	48 rpm	48 rpm	48 rpm
1	3e-5/ 450/ <b>11%</b>	8.6e-5/ 540/ <b>14%</b>	2e-5/ 370/ <b>14%</b>	3e-5/ 450/ <b>16%</b>
16	2e-5/ 110/ <b>58%</b>	2e-5/ 130/ <b>58%</b>	4e-5/ 80/ <b>79%</b>	6e-5/ 100/ <b>98%</b>
32	3e-5/ 80/ <b>70%</b>	2e-5/ 100/ <b>67%</b>	2e-5/ 60/ <b>93%</b>	1e-5/ 80/ <b>100%</b>
64	8e-5/ 60/ <b>83%</b>	9e-6/ 70/ <b>82%</b>	1e-5/ 50/ <b>93%</b>	5e-6/ 70/ <b>100%</b>

by asterisks in Table VI. In these cases, the bird clutter increased the threshold value needed to get the same  $P_{fa}$  which in turn reduced the  $P_d$  of the PIW for the HPOL radar. The impact of the bird clutter in the dataset can also be seen by comparing the threshold value of similar cases. For example, for the HPOL cases when 16 scans were averaged and the target was at 1.5 nmi, the thresholds were 100 and 120 corresponding to 48 and 60 rpm (PIW.4 and PIW.5), while for the 120 rpm (PIW.6) case a higher threshold of 160 is observed.

Regardless of the results in table VI that were affected by the bird clutter, the PIW results show that HH and VV radar systems show equal small non-moving target detection capability. Furthermore, the results at a fixed range

TABLE V. CALCULATED  $P_{fa}/Threshold/P_d$  FOR PIW.2 AND PIW.5 SCENARIOS

Run	PIW.2		PIW.5	
	1.25		1.5	
Range (nmi)	1.25		1.5	
Number of Scans used	59	77	80	103
Settings	VV	HH	VV	HH
Scans Averaged	48 rpm	60 rpm	48 rpm	60 rpm
1	3e-4/ 510/ <b>32%</b>	6e-5/ 470/ <b>35%</b>	1e-4/ 290/ <b>12%</b>	1e-4/ 410/ <b>7%</b>
16	3e-4/ 100/ <b>100%</b>	3e-5/ 100/ <b>97%</b>	8e-5/ 90/ <b>30%</b>	6e-5/ 120/ <b>36%</b>
32	6e-5/ 80/ <b>100%</b>	1.5e-5/ 80/ <b>100%</b>	6e-5/ 60/ <b>71%</b>	7e-5/ 100/ <b>44%</b>
64	4e-5/ 40/ <b>100%</b>	3e-5/ 40/ <b>100%</b>	3e-5/ 50/ <b>36%</b>	7e-5/ 65/ <b>55%</b>

TABLE VI. CALCULATED  $P_{fa}/Threshold/P_d$  FOR PIW.1 AND PIW.6 SCENARIOS

Run	PIW.1		PIW.6	
	1.25		1.5	
Range (nmi)	1.25		1.5	
Number of Scans used	57	144	95	242
Settings	VV	HH	VV	HH
Scans Averaged	48 rpm	120 rpm	48 rpm	120 rpm
1	3.3e-5/ 610/ <b>12%</b>	2.6e-5/ 520/ <b>16%</b>	7e-5/ 370/ <b>17%</b>	7e-5/ 410/ <b>10% **</b>
16	1e-5/ 95/ <b>100%</b>	1.3e-5/ 100/ <b>94%</b>	1e-5/ 90/ <b>85%</b>	6e-5/ 160/ <b>9% **</b>
32	5e-5/ 70/ <b>100%</b>	2.6e-5/ 65/ <b>100%</b>	7e-5/ 55/ <b>100%</b>	8e-5/ 100/ <b>46% **</b>
64	1e-5/ 60/ <b>100%</b>	3.5e-5/ 50/ <b>100%</b>	1e-5/ 42/ <b>100%</b>	7e-5/ 72/ <b>81% **</b>

\*\* The data is affected by sea birds

TABLE VII. RADAR SETTINGS DURING THE FRC TRIAL

Run	Start Time (GMT)	Range (nmi)	Consilium Antenna Speed (rpm)	Rutter Radar Antenna Speed (rpm)
FRC.1	13:24 - 14:18	0 to 5	80	48
FRC.2	14:20 - 14:50	5 to 0	120	48
FRC.3	15:43 - 16:14	1 to 5	60	48

consistently show that increasing the number of processed scans in the scan-to-scan integration analyses significantly improves the radar performance as shown in Tables IV, V, and VI.

B. Fast Rescue Craft

The Canadian Coast Guard (CCG) provided a 7.33 m long FRC as a radar target during the trial, manufactured by Zodiac as shown in Fig. 4. The FRC route test pattern is shown in Fig. 5. The FRC data recordings were performed at different ranges with three different antenna rotation speeds, i.e. 48, 60, and 120 rpm as shown in Table VII.

In order to calculate meaningful  $P_d$  and  $P_{fa}$  values for a moving target, the target must be analyzed over a section of its travel that is of constant range from the radar since  $P_d$  is a function of target range. To do this, the  $P_d$  and  $P_{fa}$  are calculated for the target traveling along the transverse segments only. The  $P_d$  and  $P_{fa}$  results for this trial are shown in Table VIII, Table IX, and Table X.

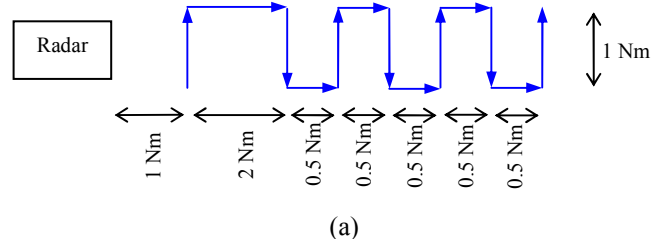
In order for scan averaging to be most effective (when used on a moving target) the target must occupy only one radar resolution cell during the period of the scan averaging. If the target moves through more than one resolution cell, the return signal gets blurred out and the signal-to-clutter ratio decreases. For a target with a constant speed, the maximum number of scans that can be averaged (number of scans that target remains in one resolution cell) depends on the antenna rotation speed. The higher the antenna rotation speed is, the greater the number of scans that can be averaged in a fixed time duration. For example, for a target at a range of 4.5 nmi moving azimuthally with the maximum speed of 25 knots, the maximum number of scans that can be integrated are 4, 5, 7, and 11 for the antenna rotation speeds of 48, 60, 80, and 120 rpm, respectively.

Fig. 6 shows the comparison between the  $P_d$  values obtained for vertical and horizontal polarizations. It is observed that vertically and horizontally polarized radars have approximately the same  $P_d$  value out to 5 nmi. But at the 5.5 nmi range (the maximum range tested), the vertically polarized radar has slightly smaller  $P_d$  value compared to the radar system with a horizontal polarized antenna. In all cases, we see that scan averaging improves the radar performance significantly. With this target and sea state we see an increase

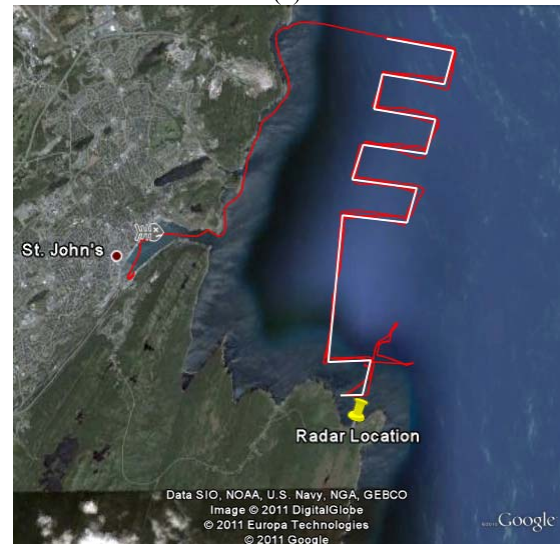


Figure 4. FRC executing trial course.

in detectable range of about 1.5 to 2.0 nmi when scan averaging is applied. The difference in  $P_d$  at larger ranges is due to the fact that the sea clutter in the VV images extends to a further distance than the HH images. Comparing the HH and VV results for all cases, it was observed that the antenna rotation speed does not improve the radar performance when no scan averaging is applied.



(a)



(b)

Figure 5. (a) FRC course during the trial. (b) Actual FRC course on the map using the GPS.

## I. CONCLUSIONS

Analysis of the results obtained for the data collected at Cape Spear show that the two radar systems (Consilium transceiver with a horizontal polarized antenna and a Rutter transceiver with a vertical polarized antenna) have very close performance in detecting the PIW and FRC targets in low sea states. The PIW results suggest that the vertically polarized antenna is just as effective for target detection as the horizontally polarized antenna in low sea states and at close range. However, in the FRC data we see the  $P_d$  value of the HH diverges from and become greater than the VV value at the furthest range. The difference in  $P_d$  at the furthest range is due to sea clutter in the VV images extending to a further distance than in the HH images.

In all cases, the scan-to-scan processing (i.e. scan averaging) significantly improved the probability of detection of the targets. For the FRC (fast target), it was theorized that a faster antenna rotation speed would allow a greater number of scans to be integrated, for the same amount of target movement, and therefore an improvement in detectability should be observed. However, the results show that the improvement is not significant. Since the trial data only included low sea states, the effect of the radar rpm on target  $P_d$  could not be fully studied. In the future, it would be useful to record FRC data at higher sea states to further study the effect of rpm on  $P_d$  for a moving target.

## ACKNOWLEDGMENT

The authors wish to thank the Canadian Coast Guard, St. John's, NL, Canada, for providing the boats and personnel for the experiments. They also thank J. Ryan, S. Hale, D. Smith, and T. Healy who provided helpful comments and suggestions, and M. Kirby for assistance with the radar data recordings. This work was supported by RDC (Research & Development Corporation Newfoundland and Labrador) R&D Proof of Concept program.

## REFERENCES

- [1] J. N. Briggs, *Target Detection by Marine Radar*. The Institute of Electrical Engineers (IEE), London, UK, 2004, p. 83.
- [2] M. W. Long, *Radar Reflectivity of Land and Sea*. 3rd ed., London: Artech House, 2001, p. 424.
- [3] M. F. Fingas, C. E. Brown, "Review of oil spill remote sensing," *Spill Science & Technology Bulletin*, vol. 4, No. 4, 1997, pp. 199-208.
- [4] M. Mityagina and A. Churumov, "Radar backscattering at sea surface covered with oil films," *EARSel: 2nd Workshop on Remote Sensing of the Coastal Zone*, Porto, Portugal, 9-11 June 2005, pp. 783-790.
- [5] A. Norris, "Civil marine radar," in *Radar Handbook*, MI Skolnik, Ed., 3rd ed., New York: McGraw-Hill, 2008, ch. 22.
- [6] J. I. Marcum, "A Statistical Theory of Target Detection by Pulsed Radar," Research Memorandum RM-753, The Rand Corporation, Santa Monica, Calif., 1948.
- [7] Sigma S6 Radar Processor, 2010. [online] Available: <http://www.rutter.ca>
- [8] C. R. Vaughn, "Birds and Insects as Radar Targets: A Review" *Proc. IEEE*, vol. 73, No. 2, Feb. 1985, pp. 205-227.

TABLE VIII.  $P_{fa}$  AND  $P_d$  CALCULATED FOR A MOVING FRC

Range (nmi)	$P_{fa}/P_d$ FRC.1					
	Scans Averaged = 1		Scans Averaged = 4	Scans Averaged = 7	Number of Scans Used	
	VPOL 48-S	HPOL 80-S	VPOL 48-S	HPOL 80-S	VPOL 48-S	HPOL 80-S
1.0	1e-5/ 100%	3e-5/ 100%	4e-5/ 100%	5e-5/ 100%	58	78
3.0	2e-5/ 99%	3e-5/ 94%	1e-5/ 100%	1e-5/ 100%	93	117
3.5	2e-5/ 95%	2e-5/ 97%	2e-5/ 100%	2e-5/ 100%	97	116
4.0	2e-5/ 89%	2e-5/ 88%	1e-5/ 100%	Data Corrupted	95	NA
4.5	2e-5/ 79%	2e-5/ 84%	1e-5/ 100%	2e-5/ 100%	95	101
5.0	1e-5/ 65%	1e-5/ 60%	2e-5/ 90%	2e-5/ 100%	108	147
5.5	1e-5/ 38%	1e-5/ 55%	4e-5/ 77%	2e-5/ 93%	124	190

TABLE IX.  $P_{fa}$  AND  $P_d$  CALCULATED FOR A MOVING FRC

Range (nmi)	$P_{fa}/P_d$ FRC.2					
	Scans Averaged = 1		Scans Averaged = 4	Scans Averaged = 11	Number of Scans Used	
	VPOL 48-S	HPOL 120-S	VPOL 48-S	HPOL 120-S	VPOL 48-S	HPOL 120-S
1.0	6e-5/ 100%	4e-5/ 100%	6e-5/ 100%	4e-5/ 100%	79	200
3.0	2e-5/ 100%	3e-5/ 100%	4e-5/ 100%	2e-6/ 100%	108	276
3.5	1e-5/ 96%	3e-5/ 93%	3e-5/ 100%	5e-5/ 100%	112	282
4.0	3e-5/ 88%	3e-5/ 91%	1e-5/ 99%	6e-6/ 100%	107	269
4.5	1.5e-5/ 77%	1.8e-5/ 72%	5e-5/ 100%	1.8e-5/ 98%	99	247
5.0	1.5e-5/ 56%	1e-5/ 54%	1.5e-5/ 90%	3e-5/ 93%	87	221
5.5	2.2e-5/ 35%	2e-5/ 44%	4.5e-5/ 76%	1.6e-5/ 91%	134	339



TABLE X.  $P_{fa}$  AND  $P_d$  CALCULATED FOR A MOVING FRC

Range (mm)	$P_{fa}/P_d$ FRC.3					
	Scans Averaged = 1		Scans Averaged = 4		Number of Scans Used	
	VPOL 48-S	HPOL 60-S	VPOL 48-S	HPOL 60-S	VPOL 48-S	HPOL 80-S
1.0	3e-5/ 100%	4e-5/ 100%	3e-5/ 100%	2e-5/ 100%	103	133
3.0	2e-5/ 99%	5e-5/ 100%	3e-5/ 100%	5e-6/ 100%	82	165
3.5	2e-5/ 98%	2e-5/ 98%	2e-5/ 100%	2e-5/ 100%	112	145
4.0	2e-5/ 88%	2e-5/ 94%	4e-6/ 100%	4e-6/ 100%	107	138
4.5	3e-5/ 77%	3e-5/ 84%	3e-5/ 100%	3e-5/ 100%	131	169
5.0	1e-5/ 73%	1e-5/ 74%	4e-5/ 98%	6e-6/ 100%	79	104
5.5	3e-5/ 47%	2e-5/ 66%	4e-5/ 83%	3e-5/ 100%	117	151

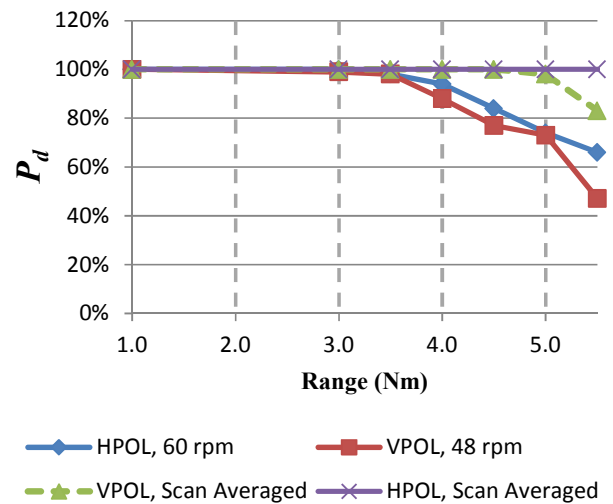
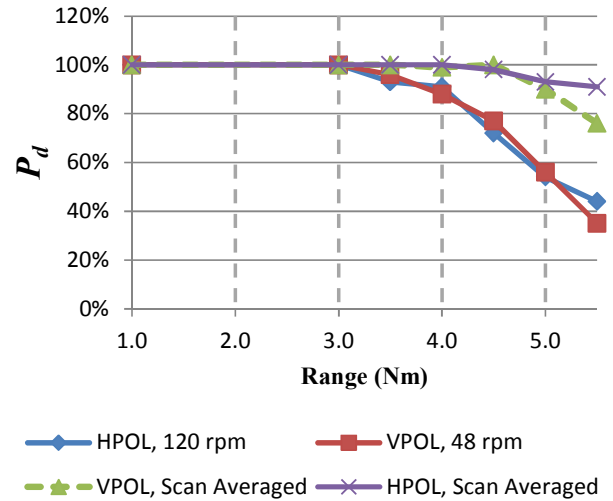
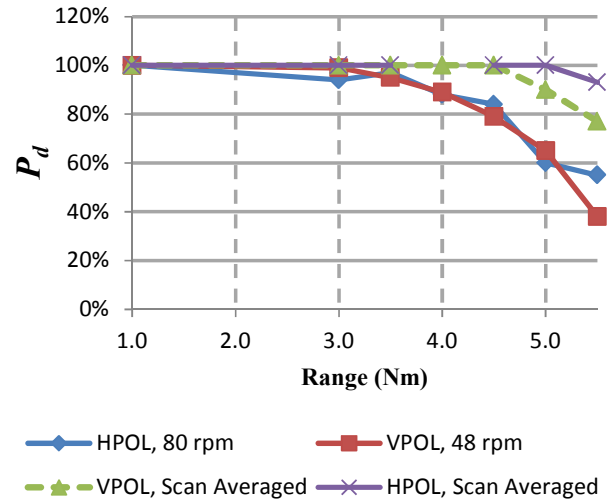


Figure 6.  $P_d$  versus range comparing vertical and horizontal polarizations for (a) FRC.1, (b) FRC.2, and (c) FRC.3. Scan averaging improves the performance for all cases.